# Parameter Identification Methods in a Model of the Cardiovascular System ⋆

**Antoine Pironet** * **Thomas Desaive** * **Pierre C. Dauby** *
**J. Geoffrey Chase** ** **Paul D. Docherty** **

* *GIGA-Cardiovascular Sciences, University of Liège, Liège, Belgium (e-mail: a.pironet@ulg.ac.be).*
** *Department of Mechanical Engineering, University of Canterbury, Christchurch, New Zealand*

**Abstract:** To be clinically relevant, mathematical models have to be patient-specific, meaning that their parameters have to be identified from patient data. To achieve real time monitoring, it is important to select the best parameter identification method, in terms of speed, efficiency and reliability. This work presents a comparison of seven parameter identification methods applied to a lumped-parameter cardiovascular system model. The seven methods are tested using *in silico* and experimental reference data. To do so, precise formulae for initial parameter values first had to be developed. The test results indicate that the trust-region reflective method seems to be the best method for the present model. This method (and the proportional method) are able to perform parameter identification in two to three minutes, and will thus benefit cardiac and vascular monitoring applications.

*Keywords:* parameter identification, mathematical models, biomedical systems, medical applications.

## 1. INTRODUCTION

Mathematical models of the cardiovascular system (CVS) can be used with clinical data to monitor cardiac and circulatory state. To be clinically relevant, these models have to be made patient-specific, which means that their parameters have to be estimated so that simulations represent a patient's individual state.

There exists two main approaches to model the CVS. The first deals with complex three-dimensional finite element models, involving millions of degrees of freedom. These models can be used to gain understanding on local parts of the CVS. The second modeling approach deals with lumped-parameter models. These models represent whole sections of the CVS as single elements (chambers or resistances, for example) and therefore involve lumped parameters reflecting the global state of a patient.

Optimising parameters of a pmodel requires a large amount of model simulations. Because of the time required to perform a single simulation of a finite-element CVS model, these models cannot currently be used to perform cardiac and circulatory monitoring. Lumped-parameter models, by their simpler nature, can be simulated much faster, which means that parameter identification can often be performed in real time.

To achieve real time monitoring using lumped-parameter CVS models, it is important to select the best parameter identification method, in terms of speed, efficiency and reliability. This work focuses on a particular lumped-parameter model and investigates seven usual parameter identification methods.

⋆ This work was supported by the French Community of Belgium, the Belgian Funds for Scientific Research (F.R.S.-FNRS) and EU Marie Curie Actions (FP7-PEOPLE-2012-IRSES).

## 2. METHODS

### *2.1 CVS Model*

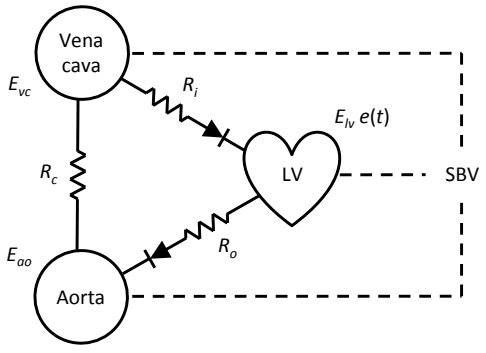


Fig. 1. Schematic representation of the CVS model.

The lumped-parameter CVS model used is presented in Fig. 1. It consists of three elastic chambers representing the left ventricle ($lv$), the aorta ($ao$) and one vena cava ($vc$). The aorta and the vena cava are described by

$$P_{ao}(t) = E_{ao}\ V_{S,ao}(t) \tag{1}$$

$$P_{vc}(t) = E_{vc}\ V_{S,vc}(t), \tag{2}$$

where $P$ is pressure, $E$ is elastance and $V_S$ is stressed volume. (Stressed volume is equal to the difference between

actual volume and a constant volume offset, called the unstressed volume.)

The left ventricle is represented using the description of Suga et al. (1973):

$$P_{lv}(t) = E_{lv}\ e(t)\ V_{S,lv}(t) \tag{3}$$

where $E_{lv}$ is the maximum (end-systolic) elastance, and $e(t)$ is the driver function, which is $T$-periodic ($T$ being the cardiac period) and ranges from 0 (end-diastole) to 1 (end-systole).

The three model chambers are linked by vessel resistances representing the systemic circulation ($R_c$), the aortic valve ($R_o$) and the whole right circulation, from the tricuspid to the mitral valves ($R_i$). Flow $Q_c$ through the systemic circulation is described by Ohm's law:

$$Q_c(t) = \frac{P_{ao}(t) - P_{vc}(t)}{R_c}. \tag{4}$$

The model assumes that (i) there is flow through the valves only if the pressure gradient is positive and (ii) that the flow through an open valve can also be described by Ohm's law. Hence,

$$Q_i(t) = \begin{cases} \dfrac{P_{vc}(t) - P_{lv}(t)}{R_i} & \text{if } P_{vc}(t) > P_{lv}(t) \\ 0 & \text{otherwise} \end{cases} \tag{5}$$

$$Q_o(t) = \begin{cases} \dfrac{P_{lv}(t) - P_{ao}(t)}{R_o} & \text{if } P_{lv}(t) > P_{ao}(t) \\ 0 & \text{otherwise.} \end{cases} \tag{6}$$

Finally, the continuity equation gives the rate at which the volume of the chambers change:

$$\dot{V}_{S,lv}(t) = Q_i(t) - Q_o(t), \tag{7}$$

$$\dot{V}_{S,ao}(t) = Q_o(t) - Q_c(t), \tag{8}$$

$$\dot{V}_{S,vc}(t) = Q_c(t) - Q_i(t). \tag{9}$$

Summing the previous equations gives:

$$\dot{V}_{S,lv}(t) + \dot{V}_{S,ao}(t) + \dot{V}_{S,vc}(t) = 0. \tag{10}$$

Consequently, the total stressed blood volume contained in the system is a constant model parameter:

$$V_{S,lv}(t) + V_{S,ao}(t) + V_{S,vc}(t) = \text{SBV}. \tag{11}$$

Overall, the model counts seven parameters (three elastances $E_{lv}$, $E_{ao}$ and $E_{vc}$, three resistances $R_i$, $R_o$ and $R_c$ and SBV) and one unknown driver function $e(t)$.

### *2.2 Available Data*

The following data was assumed to be available:

- stroke volume (SV),
- arterial pulse pressure ($\text{PP}_{ao}$),
- venous pulse pressure ($\text{PP}_{vc}$),
- mean aortic pressure (MAP),
- mean venous pressure (MVP),
- mean left ventricular volume (MLVV),
- peak first derivative of aortic pressure ($dP_{ao}/dt_{max}$),
- cardiac period ($T$),
- driver function ($e(t)$),
- onset ($t_{BS}$) and end ($t_{ES}$) of cardiac systole.

These assumptions are discussed in Section 4.4.

### *2.3 Initial Parameter Values*

Initial parameter values were obtained using the following approximations, derived in Appendix A:

$$E_{lv} \approx \frac{\text{MAP} + 0.5\ \text{PP}_{ao}}{\text{MLVV} - 0.5\ \text{SV}} \tag{12}$$

$$E_{ao} \approx \frac{\text{PP}_{ao}}{\text{SV}} \tag{13}$$

$$E_{vc} \approx \frac{2\ \text{PP}_{vc}}{\text{SV}} \tag{14}$$

$$R_i \approx \frac{\text{MVP}\ T}{2\ \text{SV}} \tag{15}$$

$$R_o \approx \frac{\int_{t_{BS}}^{t_{ES}} \left[ e(t)\ \tilde{V}_h(t)\ E_{lv} - \text{MAP} \right] dt}{\text{SV}} \tag{16}$$

with:

$$\tilde{V}_h(t) \approx \text{MLVV} - 0.5\ \text{SV} \frac{t - t_{BS}}{t_{ES} - t_{BS}} \tag{17}$$

$$R_c = \frac{(\text{MAP} - \text{MVP})\ T}{\text{SV}} \tag{18}$$

$$\text{SBV} \approx \text{MLVV} + \frac{\text{MAP}}{E_{ao}} + \frac{\text{MVP}}{E_{vc}}. \tag{19}$$

As can be seen from the equality sign in Equation 18, no approximation has been used to obtain the value of $R_c$, meaning that the value of this parameter can be exactly retrieved from the selected model outputs. This parameter was thus not included in the parameter identification procedure. The remaining parameter vector was

$$\mathbf{p} = (E_{lv}\ E_{ao}\ E_{vc}\ R_i\ R_o\ \text{SBV}). \tag{20}$$

### *2.4 Parameter Identification Methods*

Seven parameter identification methods were tested:

- the three gradient-based methods implemented in the `fmincon` function of Matlab (2014b, MathWorks, Natick, MA): active set, sequential quadratic programming (SQP) and interior point,
- the trust-region reflective (TRR) method implemented in the `lsqnonlin` function of Matlab,
- two derivative-free methods: the nonlinear simplex method of Nelder and Mead (1965) and the direct search method with random search directions and random polling (Conn et al. (2009)),
- the proportional method developed by Hann et al. (2010) for identification of lumped-parameter CVS models.

Let $\mathbf{y}$ be a vector containing the reference measurements

$$\mathbf{y} = \left( \text{PP}_{ao}\ \text{PP}_{vc}\ \text{SV}\ \text{MAP}\ \text{MVP}\ \text{MLVV}\ \left.\frac{dP_{ao}}{dt}\right|_{max} \right) \tag{21}$$

and $\hat{\mathbf{y}}(\mathbf{p})$, a vector containing the corresponding simulated values. The relative residual vector $\mathbf{r}$ between simulated and reference values was

$$r_i = 1 - \frac{\hat{y}_i(\mathbf{p})}{y_i}, \text{ for } i = 1 \text{ to } 7. \quad (22)$$

The goal of the parameter identification process was, by varying $\mathbf{p}$, to minimise the 1-norm of this vector

$$\|\mathbf{r}\|_1 = |r_1| + |r_2| + |r_3| + |r_4| + |r_5| + |r_6| + |r_7|. \quad (23)$$

Matlab was used to solve model equations and perform the parameter identification procedures. It was run on a standard laptop computer.

### *2.5 Test 1:* In Silico *Reference Data*

First, zero-noise, *in silico* reference data was generated using the four parameter sets displayed in Table 1. Parameter sets A and B produce simulations representing the hemodynamics of a patient with high (A) or low (B) cardiac contractility $E_{lv}$. Parameter set C produces simulations representing the effects of dobutamine (high contractility $E_{lv}$ and low cardiac period $T$). Parameter set D represents a case with low venous elastance $E_{vc}$.

Table 1. Reference parameter sets.

| Parameter | Units | A | B | C | D |
|---|---|---|---|---|---|
| $T$ | s | 0.8 | 0.8 | 0.5 | 1.1 |
| $E_{lv}$ | mmHg/ml | 4.7 | 1.4 | 4 | 2.6 |
| $E_{ao}$ | mmHg/ml | 1.2 | 1 | 3 | 1.4 |
| $E_{vc}$ | mmHg/ml | 0.1 | 0.2 | 0.2 | 0.008 |
| $R_i$ | mmHg s/ml | 0.04 | 0.05 | 0.04 | 0.04 |
| $R_o$ | mmHg s/ml | 0.2 | 0.05 | 0.01 | 0.02 |
| $R_c$ | mmHg s/ml | 1.5 | 1.1 | 2.7 | 3.7 |
| SBV | ml | 400 | 250 | 140 | 600 |

Let $\mathbf{p}^{\text{ref}}$ be a set of reference parameters and $\mathbf{p}[n]$, the parameter vector obtained at the $n^{\text{th}}$ iteration of the parameter identification process. The relative error vector $\mathbf{e}$ between reference and identified parameters was defined:

$$e_j[n] = 1 - \frac{p_j[n]}{p_j^{\text{ref}}}, \text{ for } j = 1 \text{ to } 6. \quad (24)$$

The total relative error between reference and identified parameters was defined as

$$\|\mathbf{e}\|_1 = |e_1| + |e_2| + |e_3| + |e_4| + |e_5| + |e_6|. \quad (25)$$

The parameter identification process was deemed successful if it recovered all of the 6 parameters with a maximum relative error below 5 %, *i.e.* $|e_j| < 0.05$ for all $j$.

### *2.6 Test 2: Experimental Reference Data*

As a second test, experimental animal data was used for parameter identification. This data came from measurements on three anaesthetised pigs, performed with the approval of the Ethics Committee of the Medical Faculty of the University of Liège. The pigs were mechanically ventilated at a positive end-expiratory pressure of 5 $cmH_2O$. Catheters (Transonic, NY) provided continuous recording of left ventricular pressure and volume and aortic pressure. SV, $PP_{ao}$, MAP, MLVV, $dP_{ao}/dt_{max}$, $T$, $e(t)$, $t_{BS}$ and $t_{ES}$ were inferred from these measurements. A PiCCO monitor (Pulsion AG, Germany) provided recording of MVP and $PP_{vc}$. Datasets E, F and G correspond to the basal state of pigs 1, 2 and 3, while dataset H was recorded on pig 3 after dobutamine infusion.

The quality of the parameter estimation was assessed using only the vector of residuals $\mathbf{r}$, since there is no reference parameter values in this case.

## 3. RESULTS

### *3.1* In Silico *Reference Data*

*Ability to Retrieve the Reference Parameters.* Table 2 summarises the outcomes of the parameter identification procedures carried out using the seven parameter identification methods on the four *in silico* reference datasets. No parameter identification method was able to retrieve the reference parameter set C. For this dataset, the proportional method performed the best and reached a total error on the parameters of 38 %. This error was almost only concentrated on the valve parameter $R_o$ (35 %), meaning that the other five parameters were correctly retrieved (see Equation 25). Despite $R_o$ not being correctly retrieved, the corresponding sum of residuals was 5 %, meaning that the valve parameter $R_o$ is practically difficult to identify.

Table 2. Result of the 28 parameter identification procedures carried out on *in silico* reference data. The letters 'Y' and 'N' indicate if the parameter identification process was able to retrieve the reference parameter set.

| | $\lvert e_j\rvert < 0.05\ \forall j$ | | | | Minimum $\|\mathbf{r}\|_1$ | | | |
|---|---|---|---|---|---|---|---|---|
| | A | B | C | D | A | B | C | D |
| Proportional | N | **Y** | N | N | 0.08 | 0.04 | 0.05 | 0.82 |
| TRR | **Y** | **Y** | N | **Y** | 0.00 | 0.00 | 0.40 | 0.00 |
| Interior point | N | **Y** | N | N | 0.08 | 0.00 | 0.14 | 0.10 |
| Active set | **Y** | **Y** | N | N | 0.00 | 0.00 | 1.59 | 0.12 |
| SQP | **Y** | **Y** | N | N | 0.00 | 0.00 | 0.57 | 0.22 |
| Simplex | N | N | N | N | 0.32 | 0.09 | 0.57 | 0.39 |
| Direct search | N | **Y** | N | N | 0.80 | 0.05 | 0.32 | 1.24 |

*Convergence Speed and Number of Function Evaluations.* Figure 2 displays the evolution of the total relative error between reference and identified parameter values $\|\mathbf{e}[n]\|_1$ during the parameter identification process carried using the reference parameter set A. As can be seen from this figure, three methods recovered the reference parameter set: TRR, active set and SQP. The proportional and interior point methods recovered all parameters with an error lower than 5 %, except the resistance of the right circulation $R_i$. The simplex method only retrieved parameters $E_v$ and SBV, and the direct search method failed to retrieve any.

Table 3 displays the time and number of function evaluations taken by the seven parameter identification methods to solve the four parameter identification problems on *in silico* reference data. According to these results, the TRR and proportional methods were the fastest.

### *3.2 Experimental Reference Data*

*Final Residuals* Table 4 displays the final $\|\mathbf{r}\|_1$ value for the seven parameter identification methods tested

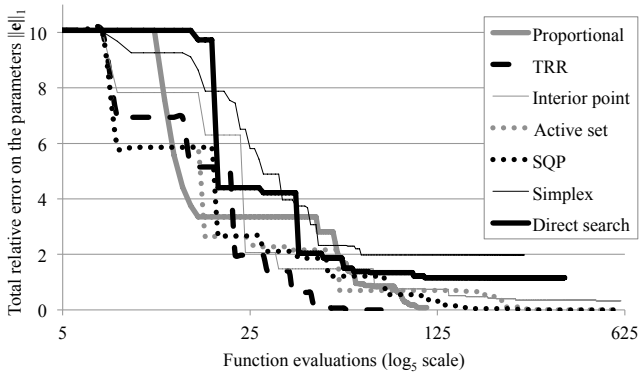


Fig. 2. Total relative error between reference and identified parameters for the seven parameter identification methods.

Table 3. Average (± standard deviation) of the time and number of function evaluations taken by the seven parameter identification methods to determine parameters for the four *in silico* reference datasets.

| | Time (s) | Evaluations |
|---|---|---|
| Proportional | $252 \pm 107$ | $97 \pm 28$ |
| TRR | $192 \pm 59$ | $63 \pm 15$ |
| Interior point | $1628 \pm 535$ | $652 \pm 84$ |
| Active set | $1041 \pm 318$ | $385 \pm 123$ |
| SQP | $995 \pm 445$ | $400 \pm 177$ |
| Simplex | $1145 \pm 829$ | $421 \pm 171$ |
| Direct search | $794 \pm 183$ | $374 \pm 128$ |

on the four experimental datasets. Overall, the gradient-based (active set, SQP, interior point and TRR) methods were able to find the lowest residuals when applied to experimental data. The proportional method performed somewhat worse than the gradient-based methods and the two derivative-free methods were the worst in finding the lowest residuals.

Table 4. Minimum norm of the residual vector for the four parameter identification problems using experimental data.

| Minimum $\|\mathbf{r}\|_1$ | E | F | G | H |
|---|---|---|---|---|
| Proportional | 0.04 | 0.29 | 2.05 | 0.03 |
| TRR | 0.02 | 0.23 | 1.65 | 0.00 |
| Interior point | 0.14 | 0.65 | 1.48 | 0.00 |
| Active set | 0.02 | 0.19 | 1.44 | 0.00 |
| SQP | 0.02 | 0.19 | 1.45 | 0.00 |
| Simplex | 0.42 | 0.64 | 2.51 | 0.00 |
| Direct search | 0.69 | 1.44 | 2.67 | 0.75 |

*Convergence Speed and Number of Function Evaluations* Table 5 displays the time and number of function evaluations taken by the seven parameter identification methods to solve the four parameter identification problems on experimental reference data. As previously, the two fastest methods are the proportional and TRR, and the two slowest methods are the simplex and interior point.

## 4. DISCUSSION

Seven methods were investigated in this work. These methods have been chosen because they are frequently applied to CVS models and/or because they are part of the widely used software Matlab. The seven methods investigated encompass the two main classes of identification methods, namely gradient-based and derivative-free methods. Five of these methods work on the norm of the residual vector, while two work on the residual vector as a whole.

Table 5. Average (± standard deviation) of the time and number of function evaluations taken by the seven parameter identification methods to determine parameters for the four experimental datasets.

| | Time (s) | Evaluations |
|---|---|---|
| Proportional | $167 \pm 52$ | $82 \pm 19$ |
| TRR | $183 \pm 54$ | $79 \pm 21$ |
| Interior point | $2127 \pm 1373$ | $1101 \pm 736$ |
| Active set | $860 \pm 198$ | $424 \pm 105$ |
| SQP | $1080 \pm 171$ | $521 \pm 49$ |
| Simplex | $2446 \pm 1124$ | $874 \pm 345$ |
| Direct search | $1172 \pm 840$ | $314 \pm 29$ |

The proportional method of Hann et al. (2010) is not always able to retrieve the parameters used to generate *in silico* reference data. It sometimes stops without having reached low residuals. However, it is one of the two fastest methods (with the TRR method), which is related to the *a priori* information required by this algorithm.

The TRR method was the most effective when applied to *in silico* reference data. It also performed quite well on experimental data. As mentioned previously, it is one of the two fastest methods (with the proportional method). Interestingly, these fastest methods are the two methods working on the error vector rather than on its norm. The good performance of the TRR method indicates that the objective function is smooth, since the TRR method approximates it with a quadratic function.

The interior point method reached average performance, both when retrieving reference parameter values and when minimizing the residuals between simulations and experimental reference data. This average performance is not compensated by speed, since this method is one of the two slowest (with the simplex method). The interior point method is known to perform worse than other gradient-based methods.

The active set and SQP methods, based on similar principles, achieved very similar results. They retrieved the reference parameters in half the cases. When applied to experimental data, they were the most efficient, since they achieved the lowest residuals. These methods have an average speed, taking approximately 15 minutes to run.

The simplex method did not retrieve any of the reference parameter sets and stopped with high residuals. It is also very time-consuming, taking 40 minutes in average when applied to experimental data. These drawbacks are inherent to the fact that this method is derivative-free.

The other derivative-free method, the direct search method, was not reliable with *in silico* reference data, and reached the highest residuals when applied to experimental data. Its speed was average.

### 4.1 Comment on Structural Identifiability

A model is structurally identifiable if and only if the residuals between reference and simulated values vanish for one and only one value of the parameters (Walter and Pronzato (1997)). This behaviour is present in Table 2, since the residuals $\|\mathbf{r}\|_1$ are close to zero if and only if the correct parameters are retrieved. This observation tends to indicate that the model is structurally identifiable. However, an exhaustive demonstration using this approach would require a test of an infinite number of parameter combinations.

### 4.2 Limitations

The results discussed in this study only apply to the CVS model presented in Figure 1. If a different model is investigated, the analysis should be repeated. To do so, the methodology can easily be transposed to another model.

The very simple CVS model used in this study represents an approximation of the reality. Such simplifications are necessary to ensure identifiability of all the model parameters. The mismatch between the model and the reality has only a small effect when using the model for monitoring cardiac and vascular state. However, predicting the effects of treatment will potentially cause larger errors because of unmodelled dynamics (for instance, nervous reflexes).

### 4.3 Preciseness of the Initial Values

To evaluate the quality of Equations 12 to 19 used to compute the initial parameter values, the initial total relative error $\|\mathbf{e}[1]\|_1$ between reference and identified parameters was assessed. Its value ranges from 133 to 1576 % (for parameter set C). Interestingly, the largest errors were again related to the valve parameters. If these errors are not considered, the total initial error on the four remaining parameters ($E_{lv}$, $E_{ao}$, $E_{vc}$ and SBV) ranges from 35 to 136 %, indicating the good preciseness of Equations 12, 13, 14 and 19.

### 4.4 Availability of the Experimental Data

First, SV can clinically be obtained using the thermodilution or echocardiography techniques. Pironet et al. (2014) recently proved it to be a necessary measurement for identification of lumped-parameter CVS models. This measurement thus had to be included in the available data.

Second, MLVV can be approximated as the mean of left ventricular end-diastolic (LVEDV) and end-systolic (LVESV) volumes:

$$\begin{aligned} \text{MLVV} &\approx 0.5\ \text{LVEDV} + 0.5\ \text{LVESV}. \\ &= \text{LVEDV} - 0.5\ \text{SV}. \end{aligned} \tag{26}$$

Pironet et al. (2015) showed that LVEDV could be derived from the measurement of global end-diastolic volume provided by cardiovascular monitoring devices using thermodilution procedures. MLVV is intuitively needed for practical identification of the heart elastance $E_{lv}$. Otherwise, there is no way of knowing the location of the pressure-volume loop on the volume axis, hence making $E_{lv}$ undetermined.

Third, systemic arterial pressure can be obtained using an arterial line. This measurement allows the computation of $\text{PP}_{ao}$, MAP, $dP_{ao}/dt_{max}$, $T$, $t_{BS}$ and $t_{ES}$, which are needed for parameter identification.

Fourth, central venous pressure is provided by a central venous line. Its mean (MVP) and amplitude ($\text{PP}_{vc}$) can then easily be obtained.

Finally, practical determination of the driver function requires simultaneous measurements of left and right ventricular pressures and volumes at different afterload levels. These measurements are not generally made in a clinical setting. However, Senzaki et al. (1996) found that the driver function was relatively similar for any human heart. This makes *a priori* generic driver functions a sensible assumption for any individual.

## 5. CONCLUSION

This work presented the comparison of seven parameter identification methods applied to a lumped-parameter CVS model. The seven methods were tested using *in silico* and experimental reference data and assessed on their speed and ability to decrease the residuals between simulations and measurements.

The TRR method seems to be the best method to recommend for the present model. Other methods that performed well are the SQP and active set, two other gradient-based methods, and the proportional method, a method that was specifically designed for the identification of lumped-parameter CVS models.

In order to test these parameter identification methods, initial parameter values had to be provided. Precise formulae were developed to achieve this goal, thereby providing the ability to speed up the parameter identification process.

Overall, this work confirmed that parameter identification in lumped-parameter CVS models can be performed in two to three minutes. Such models offer a large interest for cardiac and vascular monitoring applications.

## REFERENCES


Conn, A.R., Scheinberg, K., and Vicente, L.N. (2009). *Introduction to Derivative-free Optimization.* MPS-SIAM series on optimization. Society for Industrial and Applied Mathematics.

Hann, C., Chase, J., Desaive, T., Froissart, C., Revie, J., Stevenson, D., Lambermont, B., Ghuysen, A., Kolh, P., and Shaw, G. (2010). Unique parameter identification for cardiac diagnosis in critical care using minimal data sets. *Computer Methods & Programs in Biomedicine.*

Nelder, J.A. and Mead, R. (1965). A simplex method for function minimization. *The Computer Journal*, 7(4), 308–313.

Pironet, A., Morimont, P., Kamoi, S., Janssen, N., Dauby, P., Chase, J., Lambermont, B., and Desaive, T. (2015). Relation between global end-diastolic volume and left ventricular end-diastolic volume. *Critical Care*, 19(Suppl 1), P175.

Pironet, A., Dauby, P.C., Chase, J.G., Revie, J.A., Docherty, P.D., and Desaive, T. (2014). Structural

identifiability analysis of a cardiovascular system model. In *Proceedings of the 19th IFAC World Congress*, 3869–3874.
Senzaki, H., Chen, C.H., and Kass, D.A. (1996). Single-beat estimation of end-systolic pressure-volume relation in humans: A new method with the potential for noninvasive application. *Circulation*, 94(10), 2497–2506.
Suga, H., Sagawa, K., and Shoukas, A.A. (1973). Load independence of the instantaneous pressure-volume ratio of the canine left ventricle and effects of epinephrine and heart rate on the ratio. *Circulation Research*, 32(3), 314–322.
Walter, É. and Pronzato, L. (1997). *Identification of parametric models from experimental data*. Communications and control engineering. Springer.

## Appendix A. DERIVATION OF THE INITIAL PARAMETER VALUES

### *A.1 Left Ventricular End-Systolic Elastance $E_{lv}$*

At end-systole ($t = t_{ES}$), Equation 3 reads

$$P_{lv}(t_{ES}) = E_{lv}\ V_{S,lv}(t_{ES}) \Leftrightarrow E_{lv} = \frac{P_{lv}(t_{ES})}{V_{S,lv}(t_{ES})} \quad \text{(A.1)}$$

Assuming end-systolic cardiac pressure to be equal to systolic arterial pressure gives

$$E_{lv} \approx \frac{\text{MAP} + 0.5\ \text{PP}_{\text{ao}}}{V_{S,lv}(t_{ES})}. \quad \text{(A.2)}$$

Knowing that end-systolic cardiac volume $V_{S,lv}(t_{ES})$ is equal to minimum cardiac volume yields Equation 12.

### *A.2 Arterial Elastance $E_{ao}$*

By definition, elastance is the change in pressure caused by a change in volume. Assuming that all SV contributes to the increase in aortic pressure during systole yields Equation 13. This assumption underestimates $E_{ao}$ since some fraction of the SV actually flows through the arteries without causing an increase in pressure.

### *A.3 Venous Elastance $E_{vc}$*

Equation 9 during systole ($Q_i = 0$) reads

$$\dot{V}_{S,vc}(t) = Q_c(t). \quad \text{(A.3)}$$

Flow through the capillaries is assumed to be constant and equal to its mean value *i.e.* cardiac output, equal to $\text{SV}/T$

$$\dot{V}_{S,vc}(t) \approx \frac{\text{SV}}{T}. \quad \text{(A.4)}$$

Integrating this equation from beginning ($t_{BS}$) to end ($t_{ES}$) of systole gives

$$V_{S,vc}(t_{ES}) - V_{S,vc}(t_{BS}) \approx \frac{\text{SV}}{T}\ (t_{ES} - t_{BS}). \quad \text{(A.5)}$$

Multiplying both sides by $E_{vc}$ and using Equation 2 gives

$$P_{vc}(t_{ES}) - P_{vc}(t_{BS}) \approx E_{vc}\ \frac{\text{SV}}{T}\ (t_{ES} - t_{BS}). \quad \text{(A.6)}$$

Finally, assuming $P_{vc}(t_{ES}) - P_{vc}(t_{BS}) = \text{PP}_{vc}$ and $t_{ES} - t_{BS} = T/2$, one obtains Equation 14.

### *A.4 Resistance of the Right Circulation $R_i$*

The combination of Equations 5 and 7 during diastole ($Q_o = 0$) gives

$$\dot{V}_{S,lv}(t) = \frac{P_{vc}(t) - P_{lv}(t)}{R_i}. \quad \text{(A.7)}$$

Assuming $P_{vc}(t) \approx \text{MVP}$ and $P_{lv}(t) \approx 0$ gives

$$\dot{V}_{S,lv}(t) \approx \frac{\text{MVP}}{R_i}. \quad \text{(A.8)}$$

Integrating this equation from beginning ($t_{BD}$) to end ($t_{ED}$) of diastole gives

$$V_{S,lv}(t_{ED}) - V_{S,lv}(t_{BD}) \approx \frac{\text{MVP}}{R_i}\ (t_{ED} - t_{BD}). \quad \text{(A.9)}$$

Finally, knowing that $V_{S,lv}(t_{ED}) - V_{S,lv}(t_{BD}) = \text{SV}$ by definition of SV and assuming $t_{ED} - t_{BD} = T/2$, one obtains Equation 15.

### *A.5 Output Valve Resistance $R_o$*

Assuming that cardiac stressed volume $V_{S,lv}(t)$ ranges from MLVV + 0.5 SV to MLVV − 0.5 SV during systole allows to build a linear approximation of $V_{S,lv}(t)$ as

$$\tilde{V}_{S,lv}(t) \approx \text{MLVV} - 0.5\ \text{SV}\frac{t - t_{BS}}{t_{ES} - t_{BS}}. \quad \text{(A.10)}$$

Using this approximation and Equation 3 gives

$$P_{lv}(t) \approx E_{lv}\ e(t)\ \tilde{V}_{S,lv}(t). \quad \text{(A.11)}$$

Equation 6 during systole reads

$$Q_o(t) = \frac{P_{lv}(t) - P_{ao}(t)}{R_o}. \quad \text{(A.12)}$$

Using the approximation for $P_{lv}(t)$ and assuming that $P_{ao}(t) = \text{MAP}$, one gets:

$$Q_o(t) = \frac{E_{lv}\ e(t)\ \tilde{V}_{S,lv}(t) - \text{MAP}}{R_o}. \quad \text{(A.13)}$$

Finally, integrating this equation during systole (from $t_{BS}$ to $t_{BD}$) gives Equation 16, knowing that the integral of $Q_o$ is equal to SV.

### *A.6 Capillary Resistance $R_c$*

The integral of Equation 4 over one cardiac cycle directly yields Equation 18.

### *A.7 Total Stressed Blood Volume SBV*

Equation 11 is averaged on one cardiac cycle, giving

$$\bar{V}_{S,lv} + \bar{V}_{S,ao} + \bar{V}_{S,vc} = \text{SBV}. \quad \text{(A.14)}$$

Then, Equations 1 and 2 are also averaged, yielding

$$\bar{V}_{S,lv} + \frac{\bar{P}_{ao}}{E_{ao}} + \frac{\bar{P}_{vc}}{E_{vc}} = \text{SBV}. \quad \text{(A.15)}$$

Substituting MLVV for $\bar{V}_{S,lv}$, MAP for $\bar{P}_{ao}$ and MVP for $\bar{P}_{vc}$ results in Equation 19.